Liquid−Glassy Polymer Diffusion: Rate-Controlling Step and Diffusion Mechanism

J. Pablo Tomba,*,† José M. Carella,‡ and José M. Pastor‡

Institute of Materials Science and Technology (INTEMA), National Research Council (CONICET), University of Mar del Plata, Juan B. Justo 4302, (7600) Mar del Plata, Argentina, and Department of Physics of Condensed Matter, University of Valladolid, Paseo del Cauce s/n, (47011) Valladolid, Spain

Received December 9, 2004; Revised Manuscript Received March 11, 2005

ABSTRACT: We investigate the diffusion mechanism at a liquid−glassy polymer interphase, produced in this case between poly(vinyl methyl ether) (PVME) as the liquid polymer and polystyrene (PS) as the glassy matrix. The evolution of the interphase was directly measured by using confocal Raman microspectroscopy in the depth-profiling mode. Diffusion experiments were performed in the range 85−125 °C, with the specific purpose of encompassing the glass transition temperature (T_g) of the glassy matrix (PS, 100 °C). In this way, direct evidence about the effect of the physical state of the (glassy or liquid) PS matrix on the diffusion modes was obtained. We found that the diffusion experiments performed at temperatures below the matrix T_g (liquid−glassy polymer diffusion) are controlled by the same parameters and show the same features as those performed at temperatures above the matrix T_g (liquid−liquid polymer diffusion). Furthermore, a Fickean diffusion model developed for liquid−liquid polymer diffusion correlates precisely with the whole set of data, including liquid−glassy polymer diffusion experiments, without invoking case II diffusion theory. It is concluded that the diffusion-controlling step of the process is placed at the liquid PVME−PS interphase. These observations are in marked contrast with interpretations from other authors that used the context of case II to explain the mechanisms that control the evolution of these interphases, an idea often proposed to interpret experimental results for this polymer pair. The origin of the discrepancy is discussed.

Introduction

Diffusion of organic penetrants in amorphous glassy polymer matrices has been the focus of active research for many years. The presence of a liquid/solid polymer interface whose properties evolve with time can be found in many technological applications such as polymer blends with hard and soft components, polymers for barrier applications, lithography of microelectronics components, and drug delivery systems, among many others.

The penetration of small molecules into glassy polymer matrices has been extensively studied both theoretically and experimentally.[1−3] Under certain conditions, small-sized molecules, particularly those that swell glassy polymers, can penetrate and diffuse into polymer matrices following the case II diffusion mechanism. Thomas and Windle established the fundamental principles of case II.[1] Their work inspired some definitive experiments by Kramer and co-workers that contributed to putting the mechanism principles on a firmer footing.[2,3] In this remarkable non-Fickean diffusion mechanism, the small molecule penetration causes an osmotic pressure-driven deformation process, where the glassy polymer outer layers act as semipermeable membranes through which the small size molecules can diffuse.[1] Case II diffusion is established when the stress associated with the osmotic-driven small molecules penetration overcomes the yield stress of the glassy matrix.[3] At this point, the diffusion process is controlled by the time-dependent mechanical response of the polymer to the osmotic swelling stress at the penetrant diffusion front. The rate-controlling step of the diffusion process explains the characteristic linear sorption kinetics typically observed in case II, as demonstrated by Thomas and Windle. Remarkably, case II diffusion has been observed and reported mostly in nonsolvent−polymer systems characterized by unfavorable values of the Flory−Huggins thermodynamic interaction parameter, one of the exceptions being the results reported by Gall et al. on diffusion of toluene in glassy polystyrene.[3c]

Diffusion of large molecules, i.e., polymers in the liquid state, into glassy polymer matrices has been a less studied case. Experimental results have been reported only for miscible polymer pairs, where the Flory−Huggins thermodynamic interaction parameter is favorable.[4−9] Theoretical aspects, such as the diffusion mechanism that operates in these systems, are still under discussion. By analogy with the case of small molecules, some authors have extended the concept of case II to explain the characteristics of the liquid/glassy polymer diffusion.[5−7] Other authors have questioned this idea and have suggested that the growth mechanism for these interphases may be diffusion-controlled, similar to that observed in liquid−liquid polymer diffusion between polymers with different physical properties.[9] The main arguments against the occurrence of the case II diffusion mechanism in these cases have been pointed toward the extremely low osmotic suctions associated with the large polymer molecules, insufficient to trigger a mechanism of mechanically controlled liquid penetration.

With these ideas in mind, we studied the diffusion between liquid poly(vinyl methyl ether) (PVME) and glassy polystyrene (PS), which is outlined here. The evolution of the original liquid−glassy PVME/PS interface was directly observed by "optical sectioning" with

† University of Mar del Plata.
‡ University of Valladolid.
* To whom correspondence should be addressed. E-mail jptomba@chem.utoronto.ca or jptomba@fi.mdp.edu.ar.

10.1021/ma0474630 CCC: $30.25
Published on Web 04/15/2005

confocal Raman microspectroscopy. The diffusion experiments were performed in a temperature range that encompasses the PS glass transition temperature with the specific purpose of directly comparing diffusion rates for liquid−liquid and liquid−glassy polymer diffusion in the same polymer pair. Then, the controlling step of the diffusion process was analyzed in the context of the case II and Fickean mechanisms. It is shown that the diffusion mechanism that prevails is markedly Fickean and that all the experimental observations can be explained without involving the case II theory. Results previously published by other authors were also analyzed in the context of this framework and show that the nature of the rate-controlling step seems to be general to this type of liquid/glassy polymer diffusion.

Background

This section presents a quick overview of the standard theory describing liquid−liquid polymer diffusion and some aspects of the diffusion of small molecules in glassy polymers, particularly those related with the case II diffusion mechanism. Liquid−liquid polymer diffusion proceeds in a very similar way to the classical diffusion of small molecules and can be described in terms of Fick's laws. If both liquids are identical (self-diffusion), then their molecular mobilities match, and a single molecular weight- and temperature-dependent diffusion coefficient can be used to describe the sigmoideal diffusion profiles typically found. For the most general case, the polymers may have dissimilar mobilities, i.e., different viscosity, arising from differences in T_g or molecular weight. In this case, the low-viscosity polymer diffuses uphill gradients of local microscopic monomeric friction factor, which causes a rapid decrease in the polymer mobility along the diffusion path. To describe this experiment, more complex diffusion models based on concentration-dependent diffusion coefficients have to be employed,[10] which includes the use of bulk flow contributions in the continuity equation to account for the asymmetric liquid diffusivity.[11] The interphase chemical composition profiles predicted by these models and experimentally verified are asymmetric, with higher slopes associated with the regions of lower molecular mobility (higher local T_g).[12]

The Deborah number (D_e) is a useful scaling parameter for describing the markedly different behaviors frequently found in diffusion processes. Originally introduced by Vrentas et al.,[13] it is defined as the ratio between the characteristic relaxation time of the polymer matrix and the characteristic relaxation time for diffusion in the plasticized polymer. For experiments where $D_e \ll 1$, molecules are diffusing in what is essentially a purely viscous binary mixture where conformational changes in the polymer structure take place very quickly. Thus, the diffusion mechanism will be Fickean. The liquid−liquid polymer diffusion described above is one these cases. For systems where D_e is of the order of 1 or greater, diffusing molecules are moving in a viscoelastic binary mixture, where rearrangements of the polymer chains do not all take place immediately. The instantaneous molecular configuration differs from its equilibrium state and diffusion proceeds by the so-called anomalous non-Fickian mechanism. If $D_e \gg 1$, the diffusing molecules are moving into a medium which approximately behaves as an elastic material. This is the typical case of diffusion of small molecules into a glassy polymer. When small molecules penetrate through the polymer surface until the concentration reaches an equilibrium value, a sharp diffusion front is formed that starts to move into the polymer matrix. This process is the "induction period" and represents the beginning of case II.[2,3a]

Case II diffusion has been characterized by several specific and well-described conditions. Most of the experimental studies of case II diffusion have been conducted by putting the glassy polymer in contact with an infinite source of small penetrant molecules. The physical description for this experimental setup is simpler than for experiments conducted with a limited supply of the liquid penetrant, in which the driving forces for liquid penetration change while diffusion evolves. During the induction period, the small molecules penetrate through the surface of the glassy polymer matrix as a Fickean footstep. When the penetrant concentration at the polymer surface reaches a temperature-dependent equilibrium concentration, a sharp diffusion front is formed which moves into the polymer matrix at a constant velocity, with the Fickean tail ahead. The advancing rate of the moving front is controlled by the advancing rate of the Fickean tail, which in turn depends on the diffusion coefficient of the small molecules into the glassy matrix.

The driving force for small molecules penetration arises from the differences in its concentration with respect to its equilibrium value. In their original work, Thomas and Windle expressed this driving force in terms of the osmotic pressure π.[1−3] They stated that the mechanism of mechanically controlled penetration is initiated once π, understood as an effective pressure acting on the glassy polymer, overcomes the plastic resistance of the matrix, represented by its yield stress.[1,3] This simple and intuitive description of the problem is not rigorous, as pointed out by Argon.[14] This author has furnished an excellent and more complete description of the problem,[15] pointing out that in the context of the thermodynamics of osmosis π is a "retarding force" rather than a "driving force" for liquid penetration. In the context of this more rigorous description of the problem, Argon refers to the driving force for liquid penetration as an "osmotic suction", which can be written in a simplified way as[3b,14]

$$\Sigma = \frac{kT}{\Omega} \ln\left(\frac{\Phi_{eq}}{\Phi}\right) \tag{1}$$

where Σ is the osmotic suction, Ω is the molecular molar volume of the penetrant, Φ is the concentration of penetrant at a given place, and Φ_{eq} is its temperature-dependent value at equilibrium. When the liquid penetrant diffuses into the glassy matrix, driven by Σ, it creates a dilatational misfit. This sets up a biaxial stress field, which has deviatoric and pressure components, both of which increase in the direction of increasing liquid concentration. The pressure component acts counteracting the osmotic suction, while the deviatoric component will eventually bring the originally glassy polymer toward a generalized plastic yield.[14] When the osmotic suction overcomes the misfit-induced pressure and, at the same time, the deviatoric-induced stress overcomes the matrix yield stress, the polymer just ahead of the moving front is swollen. This swelling rate controls further penetration of the small molecules, and therefore it becomes the diffusion rate-controlling step for the whole process. This relaxation-controlled diffu-

Table 1. Characteristics of the Samples Used for Diffusion Experiments

	thin layer			thick layer		
sample	Φ^{PVME}	T_g [°C]	thickness [μm]	Φ^{PVME}	T_g [°C]	diffusion temp [°C]
85-08	0.8	−30	60	0.0	100	85
105-08	0.8	−30	72	0.0	100	105
125-08	0.8	−30	65	0.0	100	125

sion mechanism constitutes the central aspect of case II diffusion and is directly related with the anomalous (linear) kinetics of sorption observed in this type of experiment, as demonstrated by Thomas and Windle.

Case II composition profiles experimentally measured have the characteristics of steplike functions, with a sharp diffusion front that acts as a boundary between the nonswollen glassy core and the swollen (glassy or not) outer region of penetrant-plasticized polymer. Most of the mathematical models developed for case II diffusion predict penetrant profiles with these characteristics. A very good summary of the most relevant can be found in ref 14. In most of them, penetrant composition profiles are calculated from a coupled system of mass and momentum balance equations. The characteristic asymmetry arises from the large changes in diffusivity experienced by the penetrant species along the diffusion path, as predicted by the original deformation-controlled diffusion model developed by Thomas and Windle, which assumes that the elongational viscosity ahead of the moving front decreases exponentially with the increase of the penetrant volume fraction.

Experimental Section

Materials and Characterization. Polystyrene (sample P1505-St, M_n = 217 000 g/mol, M_w/M_n = 1.05) and poly(vinyl methyl ether) (sample P2219-MVE, M_n = 3850 g/mol, M_w/M_n = 1.05) were purchased from Polymer Source (Dorval, Canada). Molecular weight characterization details were provided by the maker. Glass transition temperatures (T_g) for pure polymers and PS−PVME blends were measured by differential scanning calorimetry (DSC), with a Perkin-Elmer Pyris II DSC instrument. Samples were cooled and heated from −70 °C at rates of 10 °C/min under a N_2 atmosphere. T_gs were determined as the onset of the transition.

Sample Preparation for Diffusion Experiments. Details of the samples used for the whole set of diffusion experiments, including layer compositions, layer thicknesses, and diffusion temperatures, are given in Table 1. PS−PVME blends for the bilayer samples used for diffusion experiments were prepared by freeze-drying of benzene solutions at about 10% (w/w). Antioxidant (100 ppm, Santonox, Ciba-Geigy) was added to the blends to prevent oxidation. The blends were annealed overnight under vacuum at temperatures above 120 °C, prior to the molding step, to exhaustively remove any trace of solvent. Solvent removal was verified by checking for lack of T_g changes by DSC.

Composite plates for diffusion experiments were prepared by sequential vacuum molding of a PS thick layer (500 μm thick) and a PVME-rich thinner layer (between 40 and 80 μm thick), in the form of cylindrical specimens (20 mm diameter), as detailed elsewhere.[12] Diffusion between layers of the composite plates was promoted by annealing for specified times in a temperature-controlled oven (±0.5 °C). The oven was continuously flushed with dry nitrogen to avoid oxidation of the samples. We kept the original PS−PVME interface strictly horizontal all the time to prevent the flow of the low-viscosity thin layer. The samples were periodically removed from the oven for diffusion measurements and were allowed to quickly cool back to room temperature, which virtually stops polymer diffusion, before Raman measurements were performed.

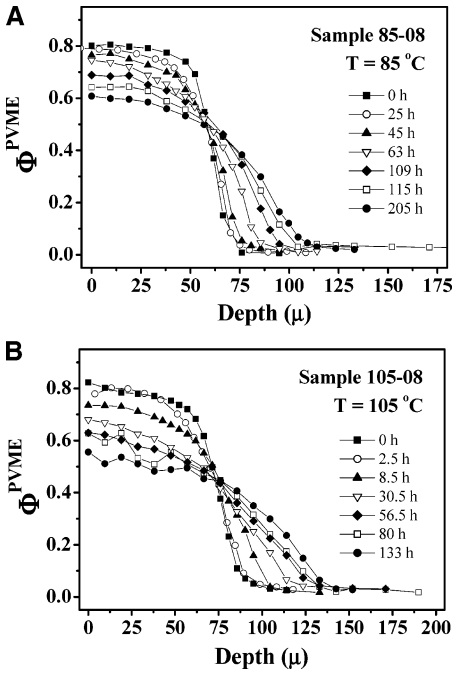

Figure 1. Typical PVME concentration profiles obtained from confocal Raman depth profiling at PVME−PS interphases for (A) sample 85-08, annealed at 85 °C for the times indicated, and (B) sample 105-08, annealed at 105 °C for the times indicated.

Confocal Raman Microspectroscopy. Local Raman spectra were measured at room temperature on a microspectrometer DILOR LabRam Confocal, equipped with a 16 mW He−Ne laser beam (632.8 nm wavelength). The pinhole opening was set between 100 and 300 μm (the maximum aperture is 1000 μm). In the excitation and collection path, an Olympus ×100 (NA = 0.9) objective was used. A slit opening of 500 μm and a holographic grating of 1800 lines/mm were used which allowed data acquisition in a Raman shifts range of 500 and 1500 cm^{-1} with a spectral resolution of 5 cm^{-1}. The acquisition time for each spectrum varied between 30 and 60 s, and 5−10 spectra were accumulated for each data point.

The technique was used in the depth-profiling mode as explained in earlier work.[12] For depth profiling, we aligned the laser beam in the direction parallel to the diffusion coordinate, and we focused it at successively deeper positions into the sample. The confocal device allows the optical sectioning of the specimen, permitting measurements for many diffusion times without altering the sample. The nominal depth resolution in our working conditions is 4 μm, but this value decreases progressively as we focus deeper into the sample, as explained in earlier work.[12] Another focusing method, surface profiling, renders superior and invariant spatial resolution but requires sample microtoming, which complicates our experimental setup.[16] For each diffusion time, the concentration profile was measured by taking several Raman spectra from different depths along the diffusion path, in steps of 2−5 μm (typically 30−40 points along the diffusion path). Local chemical compositions were calculated from the acquired Raman spectra with the linear decomposition method.[17] The procedure was repeated for several diffusion times, always focusing the laser beam within 10 μm of the same spot at the sample surface.

Results

Figure 1A,B shows representative PVME concentration profiles for diffusion experiments conducted at temperatures below and above the T_g of the PS matrix (100 °C). Figure 1A shows the volume fraction of PVME at the PVME/PS interphases of the 85-08 sample, which was annealed at 85 °C (15 °C below the PS T_g), for

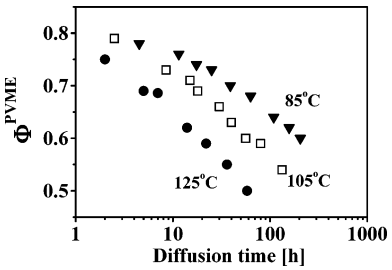

Figure 2. Chemical composition of the plateau region behind the advancing diffusion front (as PVME volume fractions) as a function of the elapsed diffusion time (logarithmic scale). Diffusion temperatures are indicated in the graph.

several time periods. Figure 1B shows the same information for the 105-08 sample, which corresponds to diffusion experiments performed at 105 °C (5 °C above the PS T_g). To obtain these concentration profiles, confocal Raman optical sectioning was started at the outer PVME surface, the zero in the depth scale axis, and then repeated at deeper positions along the PVME diffusion path.

As time increased, the limited supply of PVME advances toward the pure PS layer. All the experimental profiles show a plateau next to the outer PVME-rich layer. Moving along the diffusion path, the PVME concentration profile is at first fairly flat along the outer 50−75 μm, and then its slope becomes increasingly higher and the PVME concentration decreases rapidly, until the depth of the pure PS is reached. The limited PVME supply causes the PVME concentration at the plateau region to decrease with diffusion time. In our experiments, the transition from the PVME-rich region to the glassy PS layer appears artificially smoothed over a region of tens of microns in the depth scale due to limitations in the spatial resolution of the depth-profiling confocal Raman technique.[12,16,18] In previous work, we have shown that the tails observed to the right-hand side of the highest slope region in the diffusion profiles are artifacts generated by the focusing method used for Raman measurements.[16,18] When we studied these interphases with a focusing method with superior and invariant spatial resolution (surface profiling), we found that the transition from the rich PVME to the pure glassy PS phase is abrupt and occurs in a narrow range on the depth scale (1−2 μm). No tails in the pure PS phase were detected in the scale of the spatial resolution of the method (1.5 μm).[16,18] Thus, the real PVME profiles can be though as having a plateau region with uniform PVME concentration followed by a sharply defined drop in concentration with the characteristics of a diffusion front.

Figures 2 and 3 present a series of plots that characterize the diffusion kinetics in the PVME/PS polymer pair. Figure 2 shows the evolution of the PVME concentration at the plateau region, behind the diffusion front, as a function of the diffusion time. The plateau region coincides with chemical compositions that correspond to the highest polymer mobility, and its time evolution is very sensitive to the features that control the diffusion process. The experimental data shown correspond to averaged values for the outer 50 μm of the PVME-rich layer, and these have been represented using a different symbol for each diffusion temperature.

Another parameter frequently used to characterize diffusion mechanisms is the time evolution of the diffusion front position and its instantaneous velocity.

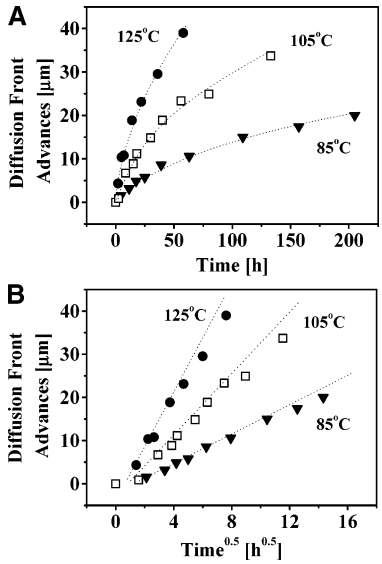

Figure 3. Kinetics of the advancing diffusion front for experiments performed at 85, 105, and 125 °C. Advances of the diffusion front (A) as a function of the elapsed time and (B) as a function of the square root of the elapsed time.

As mentioned above, instrumental artifacts make the precise localization of the diffusion front difficult in our system. On the other hand, the plateau region is almost insensitive to effects of instrumental broadening because the lower slopes in this region are much less affected by the enlargement of the volume over which the Raman signal is effectively averaged. We can take advantage of the fact that the PVME concentration profiles look almost like a rectangular box[12] and that the mass conservation requires the area under the concentration profile to be a constant. Therefore, the PVME advancing front positions into the glassy PS layer can be directly calculated from the plateau concentration value and the area under the profile. This procedure, also employed by other authors,[7] will be used throughout this paper to obtain the time evolution of the diffusion front. The results are plotted in Figure 3A,B. The aim of Figure 3A is to explore the advancing diffusion front positions in the context of the case II diffusion theory, showing the successive front positions as a function of annealing time. Figure 3B shows the same plot in the Fickean fashion as a function of the square root of the elapsed diffusion time.

Discussion

Diffusion Profiles and Kinetics of Interfacial Mixing. We begin with an examination of the characteristic features of the diffusion profiles in terms of shape and symmetry. The PVME concentration profiles shown in Figures 1A,B are asymmetric. The volume fraction of PVME is fairly constant in the plasticized region (high PVME volume fraction) behind the diffusion front and then drops off sharply ahead of it. For experiments conducted at 125 and 105 °C, the diffusion temperature is above the T_g of the PS matrix, which behaves like a highly viscous liquid during the whole experiment. These cases can be thought as diffusion of low-viscosity PVME into a highly viscous PS matrix, and the asymmetry of the profiles can be explained in terms of the dissimilar mobility of PVME and PS.[12]

In the experiments conducted at 85 °C, the PVME concentration profiles are also asymmetric and look

qualitatively similar to those observed at 105 and 125 °C. The fundamental difference with those experiments is that at this diffusion temperature (85 °C) the PS layer remains glassy during the whole process. Asymmetric liquid profiles produced by diffusion in a polymer layer that remains glassy at the temperature of the experiment is a condition usually found in diffusion mechanisms controlled by mechanical relaxation, and it would be tempting to consider this experiment as an example of case II. However, this condition is not sufficient for the occurrence of case II, and more experimental evidence along with a careful analysis of the kinetics of mixing are required to confirm the diffusion mechanism that operates in this case.

The dependence of the PVME diffusive transport on chemical composition can be analyzed from the results of Figure 2, which shows the evolution of the PVME volume fraction at the plateau region with elapsed diffusion time and penetration depth. The slopes observed in each of these curves reflect the dependence of the parameters that control the diffusion process on composition or diffusion time, as has been discussed in refs 7 and 9. Remarkably, the data show the same trend for experiments performed below and above the PS T_g, despite the dramatic differences in the physical state of the PS matrix. This fact indicates that the parameters that control the PVME diffusive transport and their dependence on composition are the same for both experiments. Some authors have used this type of plot to analyze changes in the diffusion mechanism with the plasticized layer composition. Nealey et al.[7] studied the diffusion of a plasticizer (resorcinol bis(diphenyl phosphate) (RDP)) into the glassy engineering thermoplastic ULTEM in a temperature range between 95 and 55 °C below the ULTEM T_g. The RDP−ULTEM system shows remarkable similarities with our experiments in the sense that the RDP molecule, with a molar volume comparable to that of our PVME molecule, is completely soluble in the ULTEM matrix and also diffuses from a limited supply source. The authors observed that at intermediate volume fractions of RDP the slope of the plot changes abruptly (see Figure 13 of the mentioned work), which they ascribed to changes in the diffusion mechanism, from case II at short times to anomalous diffusion at long times. However, only qualitative explanations in terms of the Deborah number were given to support this argument. In our experiments, that nicely encompass a wide range of diffusion times (and diffusion rates), we did not observe any abrupt changes of slope that may support changes in the diffusion mechanism associated with variations of the plasticized layer composition.

The time scaling laws for the diffusion front propagation are examined in Figure 3. Figure 3A shows that for all our experiments the displacement of the PVME diffusion front that advances into the pure PS matrix is markedly nonlinear with time. This fact is not surprising for the experiments conducted at 125 °C, for which diffusion is expected to be Fickean. The marked deviation of the front position from a linear scaling law observed in the experiment at 85 °C does not give support for a case II mechanism, as one of the characteristic signatures of this mechanism is the linear propagation of the diffusion front with time, which originates in the coupling between diffusion and mechanical relaxation.[1] One may argue that this apparent nonlinearity could arise from the boundary condition of our experiments. In limited-supply conditions, the PVME volume fraction in the plateau region decreases with time and penetration depth. Therefore, the local driving force (osmotic suction or concentration gradients) changes continuously with time and depth. In contrast, under an infinite supply boundary condition, i.e., the penetrant supply is unlimited, a fully developed diffusion front propagates under a constant driving force with a constant velocity because the properties of the plasticized layer are constant. Theoretical studies of case II diffusion by Hui et al.[2] and Argon et al.[14] have shown that at high penetrant concentrations, as in our case, the diffusion front velocity is relatively insensitive to changes in the concentration of the plasticized layer. We believe that even for a limited supply experiment, an almost linear relationship should be observed for the experiment performed at 85 °C, if the diffusion was controlled by a case II mechanism.

Remarkably, all the data scale very closely with $t^{1/2}$, a typical signature of Fickean diffusion, as observed in Figure 3B. Only at very long diffusion times is a downward curvature observed in all the experiments. As will be shown later, it is due to changes in the diffusion coefficients as diffusion evolves, which is a typical signature of liquid−liquid diffusion between components with different T_g. It suggests that the transport of PS into the PVME layer is Fickean in all the cases, including the experiment performed at 85 °C.

Comparison with Other Similar Diffusion Experiments. Examination of the most relevant results on liquid/solid polymer diffusion published in the literature shows that Fickean kinetics of mixing is expected to be general. Composto et al. studied the diffusion of liquid PS into a glassy poly(phenylene oxide) (PPO) matrix at temperatures between 6 and 39 °C below the PPO T_g, using Rutherford backscattering spectrometry (RBS).[4] Markedly asymmetric PPO concentration vs depth profiles were measured, with a low slope at low values of PPO volume fractions and a much greater slope at high values of PPO volume fractions. The diffusion front was sharp, and no Fickean tails were reported. All these features coincide with our experimental findings. The authors observed that the displacement of the interface followed a $t^{1/2}$ scaling law. A close inspection to the data (Figure 8, ref 4) reveals that the plots are not strictly linear and show the same type of downward curvature observed in our experiments.

In another study Feng et al. used neutron reflectivity to probe the interfacial mixing between the poly(*N*,*N*-dimethylethylenesebacamide)−polystyrene ionomer (mPA/Li−PS) polymer pair.[8] The diffusion experiments were conducted at 96 °C, which is 24 °C below the glass transition temperature of the low-T_g polymer (Li−PS, T_g = 120 °C), while the mPA component was a liquid at this temperature (T_m = 75 °C). They observed that at short diffusion times the interface moved toward the Li−PS, following a $t^{1/2}$ scaling law consistent with a Fickean mechanism. A deviation in the form of a downward curvature was observed at longer times, attributed to a dramatic slowing down of the diffusion process due to the formation of strong hydrogen bonds between components, which prevents further diffusion.

We have studied in our lab the diffusion of oligomeric PS into glassy PPO using the same experimental technique described in this work. The low T_g of the PS used allowed the study of diffusion at temperatures well below the T_g of the glassy matrix (between 60 and 100

°C below the PPO T_g), which is otherwise difficult to access.[18] The whole set of experimental data, which included PS concentration profiles and diffusion kinetics, were consistent with predictions of a Fickean diffusion model. Only the experiments performed at 100 °C, in which we observe a remarkable slowdown of polymer diffusion, did not follow the model prediction, which was suggested to be due to thermodynamic factors.

The only exception to this general behavior, which partially motivated the present work, are the experiments reported by Sauer et al. on the PS−PVME pair.[5] These authors investigated the diffusion between PVME and a glassy PS matrix at 24 °C below the PS T_g, using a combination of neutron reflection and spectroscopic ellipsometry. The PVME used was a high molecular weight sample (M_w = 99 000 g/mol, M_w/M_n = 2) while the PS had a molecular weight comparable to that used here. The PVME also diffused from a finite layer in the form of limited supply. In fact, the PVME volume fraction in the rich PVME layer decreased throughout the experiments from 1.0 to 0.84. The authors observed that the advancing diffusion front followed an apparently linear dependence with time and that asymmetric PVME concentration profiles produced a better fit of their experimental data. On the basis of these observations, they concluded that the penetration of PVME into the glassy PS matrix followed case II diffusion mechanism. However, as has been shown here, the asymmetry of the liquid-penetrant composition profile can be explained without invoking case II. In our understanding, the apparent linear kinetic of mixing observed in these experiments is due to the relatively narrow range of diffusion times/plateau concentrations studied, which does not allow to distinguish between linear and square root time dependence. Sound arguments against the occurrence of the case II mechanism in liquid−glassy polymer diffusion, particularly if the liquid polymer has a high molecular weight, will be given in the next section.

Liquid−Liquid and Liquid−Glassy Diffusion Controlled by a Common Step. The experiments performed at temperatures above and below the glass transition of the glassy matrix provide a unique tool for the exploration of the effects of matrix properties on diffusion behavior at these liquid/glassy polymer interphases. Going from diffusion experiments conducted at 25 °C above the PS T_g to 15 °C below the PS T_g produces dramatic changes in the relaxation rate of the PS matrix. From the mechanistic point of view, this fact ought to affect the way that the liquid PVME penetrates into the PS glassy matrix, if that hypothetical process was controlled by the mechanical relaxation of the glassy matrix. However, there are no indications of change in the diffusion mode despite the dramatic change in the physical state of the PS matrix. The data analyzed so far indicate that (a) the experiment conducted at 85 °C, well below the matrix T_g, is controlled by the same parameters that control the experiments conducted above T_g, which necessarily involve liquid−liquid polymer diffusion, and (b) the kinetics of mixing observed has more likely characteristic of Fickean diffusion than that observed in case II.

Further support for a Fickean diffusion mechanism can be obtained by comparing the experimental data of this work with predictions from models for liquid−liquid polymer diffusion. We have shown that the diffusion at

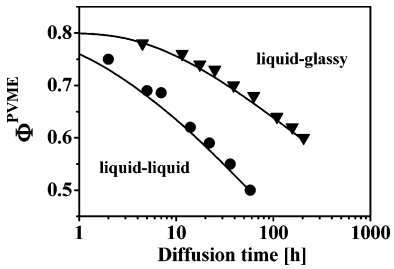

Figure 4. Comparison of the diffusion model prediction to the experimental data. The symbols correspond to experimental PVME volume fractions at the plateau region and the solid lines to model predictions. Liquid−glassy diffusion refers to diffusion experiments performed at 85 °C; liquid−liquid refers to experiments performed at 125 °C.

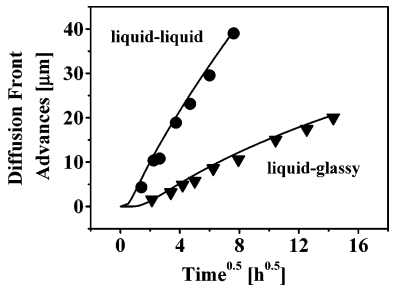

Figure 5. Comparison of the diffusion model prediction to the experimental data. The symbols correspond to experimental advances of the diffusion front, plotted in Fickean fashion, for the same experiments shown in Figure 4. The solid lines represent model calculations.

liquid−liquid PVME−PS interphases can be precisely described using a Fickean model with a variable diffusion coefficient. Full details of this model and the parameters used for the numerical simulations have been published elsewhere,[12] and here we summarize its main characteristics. The flux of the individual components is expressed following the Onsager formalism as the product of a kinetic factor, associated with the mobilities of each component, and a thermodynamic factor related to the individual gradients of chemical potential. The kinetic factor is expressed in terms of the monomeric friction coefficients of each component, which were obtained from independent tracer diffusion experiments.[19] Changes in the monomeric friction coefficients with free volume are calculated with the Williams−Landel−Ferry equation.[19] The thermodynamic factor is derived from the Flory−Huggins theory, and it is expressed as a function of distributions of molecular weights for each component and the Flory−Huggins interaction parameter for the system.[20] A bulk flow, typical for systems with asymmetric diffusivities, is also included in the transport equations.[21] The model predicts asymmetric PVME concentration profiles with the characteristics reported here. The PVME profiles are flat in the regions of low viscosity (high PVME concentration), and then their slope becomes very steep when approaching the highly viscous matrix (PS). The changes in the concentration profile slope are associated with the rapidly changing T_g profile along the diffusion path.[12]

The model predictions are compared with the experimental data in Figures 4 and 5 for experiments conducted well above (125 °C) and below (85 °C) the T_g of the PS matrix. Figure 4 shows the evolution of the PVME volume fraction at the plateau region with the elapsed diffusion time. Figure 5 shows the advancing

diffusion front kinetics plotted in Fickean fashion as a function of $t^{1/2}$. The model predictions are shown in the figures as solid lines and the experimental data with symbols. In Figure 5, we obtained the diffusion front advances predicted by the model from the PVME concentration at the plateau region and the area under the profile, the same methodology employed to obtain the front advances from the experimental data. The model predicts remarkably well and with the same precision the experiments conducted at temperatures above the matrix T_g, which we refer to as liquid−liquid polymer diffusion, and those performed below T_g, referred to as liquid−glassy polymer diffusion. As has already been shown in previous work, the model also predicts correctly the shape of the PVME composition profiles experimentally measured.[12]

We understand that these results strongly suggest that the diffusion-controlling step is the same for both liquid−liquid and liquid−solid polymer interphases. In this scenario, we rationalize the series of events that allow a single PS chain to travel toward the PVME-rich liquid as follows: First, the chain must acquire enough mobility to diffuse, and this step may only be accomplished by dissolving it with enough PVME to reach a solution T_g lower than the temperature of the experiment. The dissolution process is favored by negative values of the thermodynamic interaction parameter for the system[6,20] and by the low molecular weight of the PVME. Once the PS chain is in the liquid state, it can then diffuse down a combination of two gradients: PS concentration and local T_g. The combination of two gradients in the same direction causes a very rapid increase in the PS chain mobility. As shown in earlier work, the mobility of the PS chains in this polymer pair changes by orders of magnitude along the liquid diffusion path.[12] At the same time, it makes clear why the controlling step for the process occurs at the liquid-phase zone with the highest T_g. Considering that the dissolution of the PS chains involves only small-scale movements in the PVME chains and, conversely, the translation of PS chains involves large-scale cooperative center-of-mass movements in an extremely viscous medium, we can now understand why the dissolution process can provide all the PS chains that can then diffuse away. Furthermore, the monomeric friction coefficient for PVME is much smaller than for PS,[12] and therefore small-scale movements for PVME chains will be much faster than large-scale cooperative PS movements. Thus, these diffusion processes at temperatures above and below the PS matrix T_g are controlled by a common step.

We end this section with some comments about why the case II mechanism should not be expected to control the dissolution process at liquid/glassy polymer interfaces, an idea we introduced in previous work.[9] As explained earlier, the distinctive characteristic of the case II mechanism is its rate-limiting step controlled by the mechanical relaxation of the glassy polymer. One of the necessary conditions for this type of control is that the osmotic suction overcomes the misfit-induced pressure produced by the presence of the liquid penetrant in the glassy matrix. This osmotic suction, as calculated from eq 1, depends inversely on the molar volume of the penetrant molecule Ω, which in turn can be expressed as MW/δ, where MW is the penetrant molecular weight and δ its density. For example, compared at the same composition gradients, the polymer used in this work (PVME $M_n \sim 4000$ g/mol, $\delta \sim 0.96$ g/mL) produces an osmotic suction 40 times smaller than that exerted by a small molecule such as toluene (MW = 92 g/mol, $\delta \sim 0.87$ g/mL). That value is 125 times smaller than the osmotic suction associated with the methanol (MW = 32 g/mol, $\delta \sim 0.79$ g/mL) used in the experiments of Thomas and Windle. For the polymer used in the experiments of Walsh et al. referred to in the previous section (PVME $M_n \sim 50\,000$ g/mol), the osmotic suction is expected to be 540 times smaller than that produced by toluene or 1500 times smaller than that for methanol. Clearly, large molecules as liquid polymers generate osmotic suctions orders of magnitude smaller than those produced by small-sized penetrants. On the other hand, it has also been established that the Fickean precursor formed ahead of the advancing front in case II diffusion plays an important role in plasticizing the glassy matrix, which additionally contributes to reducing its yield stress.[2,3] The relative size of the Fickean precursors depends, among other factors, on the value of the diffusion coefficients of the liquid penetrants into the glassy matrix, which are expected to be extremely low for large-sized liquid polymers. The absence of significant Fickean tails observed in previous experiments involving large liquid/glassy polymer interphases confirms this assumption.[4,18] We believe that the combination of these factors, low osmotic suctions and low efficiency in decreasing the plastic resistance of the glassy matrix, which are both associated with the large molar volume of the liquid, prevents the triggering of a mechanism controlled by the mechanical relaxation of the glassy matrix.

Conclusions

This paper has demonstrated that the transport mechanism at the liquid PVME/glassy PS polymer interface is controlled by a liquid−liquid diffusion step rather than by a process of mechanical deformation with case II characteristics, as observed in the diffusion of small molecules in glassy polymers. Discrimination between this physical interpretation and that corresponding to case II was achieved by focusing on specific aspects of the process. We have shown that dramatic changes in the physical state of the matrix, from the glassy to the liquid state, do not affect the diffusion mechanism. At any temperature, and independently of the state of the matrix, the PVME transport into the PS matrix was markedly Fickean. Finally, all the diffusion experiments were fully described by a diffusion model developed for liquid−liquid polymer diffusion, with no considerations about the coupling between the mechanical response of the glassy polymer and the liquid diffusion.

The PVME/PS pair was not a fortuitous choice for these studies. In some ways, this polymer pair has been considered for a long time a classic example of case II diffusion in liquid−glassy polymer interfaces.[5,6,22] The results of our work have shown that this may not be the case and raise some issues related with the analysis of the evidence for occurrence of the case II mechanism. It has to include the analysis of the shape of the liquid diffusion profiles, the study of the kinetics of mixing in extended range of diffusion times, and the use of suitable diffusion models for data interpretation.

Even though we have used the PVME/PS system to exemplify the case, we believe that the ideas and the diffusion mechanism presented in this work are general

for liquid/glassy polymer interfaces. Because of the negligible osmotic suctions generated at the interface and the low diffusion coefficients associated with large liquid polymer molecules, the conditions for case II are, from our point of view, difficult to meet at liquid/glassy polymer interphases. We hope these ideas stimulate more work in the field that contributes to a definitive understanding of the mechanisms of diffusion at liquid−glassy polymer interphases.

Acknowledgment. Financial support from "Agencia Nacional de Promoción Científica y Tecnológica" (ANPCYT-PICT 14-07247), from "Programa de Cooperación con Ibero-América" (BOE 29.2.2000), and from CYTED (Project VIII-11) made this research work possible. J. P. Tomba thanks Robert R. Roller for proofreading the manuscript.

References and Notes

(1) (a) Thomas, N. L.; Windle, A. H. *Polymer* **1980**, *21*, 613. (b) Thomas, N. L.; Windle, A. H. *Polymer* **1981**, *22*, 627. (c) Thomas, N. L.; Windle, A. H. *Polymer* **1982**, *23*, 529.
(2) (a) Hui, C.-Y.; Wu, K.-C.; Lasky, R. C.; Kramer, E. J. *J. Appl. Phys.* **1987**, *61*, 5129. (b) Hui, C.-Y.; Wu, K.-C.; Lasky, R. C.; Kramer, E. J. *J. Appl. Phys.* **1987**, *61*, 5137.
(3) (a) Lasky, R. C.; Kramer, E. J.; Hui, C.-Y. *Polymer* **1988**, *29*, 673. (b) Gall, T. P.; Lasky, R. C.; Kramer, E. J. *Polymer* **1990**, *31*, 1491. (c) Gall, T. P.; Kramer, E. J. *Polymer* **1991**, *32*, 265.
(4) Composto, R. J.; Kramer, E. J. *J. Mater. Sci.* **1991**, *26*, 2815.
(5) Sauer, B. B.; Walsh, D. J. *Macromolecules* **1991**, *24*, 5948.
(6) Jabbari, E.; Peppas, N. A. *Macromolecules* **1993**, *26*, 6229.
(7) Nealey, P. F.; Cohen, R. E.; Argon, A. S. *Polymer* **1995**, *36*, 3687.
(8) Feng, Y.; Weiss, R. A.; Karim, A.; Han, C. C.; Anker, J. F.; Kaiser, H.; Peiffer, D. G. *Macromolecules* **1996**, *29*, 3918.
(9) Tomba, J. P.; Carella, J. M.; García, D.; Pastor, J. M. *Macromolecules* **2001**, *34*, 2277.
(10) (a) Kramer, E. J.; Green, P. F.; Palmstrom, C. J. *Polymer* **1984**, *25,* 473. (b) Composto, R. J.; Kramer, E. J.; White, D. M. *Macromolecules* **1988**, *21*, 2580.
(11) Tomba, J. P.; Carella, J. M. *J. Polym. Sci., Polym. Phys. Ed.* **1999**, *37*, 3097.
(12) Tomba, J. P.; Carella, J. M.; García, D.; Pastor, J. M. *Macromolecules* **2004**, *37*, 4940.
(13) Vrentas, J. S.; Jarzebski, C. M.; Duda, J. L. *AlChE J.* **1975**, *21*, 894.
(14) Argon, A. S.; Cohen, R. E.; Patel, A. C. *Polymer* **1999**, *40*, 6991.
(15) Reference 14 includes not only an excellent description of the driving forces involved in the diffusion processes of small molecules into glassy polymeric matrices but also a rigorous description of the deformation process that takes place in the glassy matrix.
(16) (a) Everall, N. J. *Appl. Spectrosc.* **2000**, *54*, 773. (b) Everall, N. J. *Appl. Spectrosc.* **2000**, *54*, 1515.
(17) Tomba, J. P.; De la Puente, E.; Pastor, J. M. *J. Polym. Sci., Part B: Polym. Phys.* **2000**, *38*, 1013.
(18) Tomba, J. P.; Carella, J. M.; Pastor, J. M.; Merino, J. C. *Polymer* **2002**, *43*, 6751.
(19) (a) Green, P. F. *Macromolecules* **1991**, *24*, 3373. (b) Green, P. F.; Adolf, D. B.; Gilliom, L. *Macromolecules* **1991**, *24*, 3377.
(20) Hammouda, B.; Briber, R. M.; Bauer, B. J. *Polymer* **1992**, *33*, 1785.
(21) The bulk flow mentioned here is analogous to the vacancy flux introduced in the original Kramer's model (ref 10a).
(22) Vaudreuil, S.; Qiu, H.; Kaliaguine, S.; Grmela, M.; Bousmina, M. *Macromol. Symp.* **2000**, *158*, 155.

MA0474630